

Effect of Notch Severity on Thermomechanical Fatigue Life of a Directionally-solidified Ni-base Superalloy

Patxi Fernandez-Zelaia¹ and Richard W. Neu^{1,2*}

¹ Woodruff School of Mechanical Engineering, Georgia Institute of Technology, Atlanta, Georgia, 30332, USA

² School of Materials Science and Engineering, Georgia Institute of Technology, Atlanta, Georgia, 30332, USA

* Corresponding author: rick.neu@gatech.edu

Abstract The aim of this research is to understand the influence of notches under thermomechanical fatigue (TMF) in a directionally-solidified (DS) Ni-base superalloy. Experiments were performed utilizing linear out-of-phase (OP) and in-phase (IP) TMF loadings on longitudinally-oriented smooth and cylindrically-notched specimens. Several notch severities were considered with elastic stress concentrations ranging from 1.3 to 3.0. The local response of the notched specimens was determined using the finite element method with a transversely isotropic viscoplastic constitutive model. Comparing the analysis to experiments, the locations observed for crack nucleation in the notch, which are offset from the notch root in DS alloys, are consistent with the maximum von Mises stress. Various local and nonlocal methods are evaluated to understand the life trends under OP TMF. The results show that a nonlocal invariant area-averaging method is the best approach for collapsing the TMF lives of specimens with different notch severities.

Keywords notched specimens, thermomechanical fatigue, Ni-base superalloy, notch analysis

1. Introduction

Components in the high pressure turbine section of gas turbine engines undergo complex thermomechanical loads during engine cycle transients. Turbine blades contain stress elevating features such as cooling holes or fir-trees that can have a detrimental effect on component endurance and make endurance prediction difficult. The surrounding material around these stress elevators undergo cyclic inelastic deformation providing a source for fatigue crack nucleation [1, 2]. To improve component level endurance prediction methodologies, the effect of stress elevators on thermomechanical fatigue (TMF) needs to be addressed.

Few studies have targeted the problem of determining crack initiation of notched specimens under TMF. Presently, no accepted methods exist for predicting TMF crack initiation life at notches. Studies on the TMF of circumferentially-notched specimens fabricated from a rotor steel, 1CrMoV, found that uniaxial life results could be used to predict the notch endurance given that conditions at the notch root were comparable [3, 4]. Large spatial gradients were shown to reduce the driving force for creep damage and fatigue crack growth away from the notch root in notched specimens. For identical crack initiation criteria, this effect could potentially increase the measured endurance as physically small cracks grow slower in notched specimens.

A study on the TMF of notched specimens of Ni-base superalloys by Kupkovits and Neu [5] found that damage mechanisms present in notched specimens are identical to smooth specimens. Notched specimen geometries corresponding to theoretical elastic stress concentration factors of $k_t = 2$ and $k_t = 3$ were studied. Under $500^\circ\text{C} \leftrightarrow 950^\circ\text{C}$ OP TMF conditions loaded in the longitudinal (L) orientation, the reduction in life was identical for both of these notches in contrast to isothermal fatigue where the more severe notch had a greater knockdown factor [6]. The same held true under $500^\circ\text{C} \leftrightarrow 750^\circ\text{C}$ OP TMF. Fatigue-environmental damage mechanisms were observed in notched OP TMF $500^\circ\text{C} \leftrightarrow 950^\circ\text{C}$. All notched specimen experiments resulted in crack nucleation at the location of maximum Hills' or von Mises equivalent stress similar to isothermal fatigue studies [6].

This work identified the need to explore the TMF life behavior of less severe notches geometries to understand the transition in fatigue behavior from smooth specimens ($k_t = 1$) to the more severely notched specimens ($k_t \geq 2$).

This paper focuses on the role of notch severity on TMF life expanding the work described in Kupkovits and Neu [5] by considering milder notches. The notch response is evaluated using a transversely isotropic viscoplasticity model to further understand the gradients in the cyclic stress-strain response that influence of notch severity on life. Local and several nonlocal methodologies for life assessment are evaluated to determine which approaches exhibit the most promise for assessing notches under TMF.

2. Methods

2.1. Smooth and notched specimen experiments

One cylindrical smooth specimen ($k_t = 1$) and four different cylindrically-notched specimens ($k_t = 1.3, 1.7, 2$ and 3 based on isotropic elastic behavior) were utilized in TMF experiments. The net section diameter for all notched specimens was 6.35 mm , same as the diameter of the smooth specimen. The outside diameter for all notched specimens was 9.53 mm .

2.2. Material

The DS Ni-base superalloy, with primary alloying elements (in wt. %) 0.07C, 8.1Cr, 9.2Co, 9.5W, 3.2Ta, 0.5Mo, 5.6Al, 0.7Ti, 1.4Hf, was received in cast slabs consisting of columnar grains in the long direction of each slab with grain diameter varying from $200 \mu\text{m}$ to 1 mm with an average grain diameter of 0.5 mm . A standard heat treatment was applied to the slab to produce a microstructure representative of an in-service blade material. The microstructure consists of FCC matrix (γ) containing cuboidal γ' precipitates. The γ' in the as-received and heated-treated material had an average volume fraction of 60% and a bi-modal size distribution of cuboidal 500 nm and fine secondary precipitates in the γ channels of 75 nm in size.

All specimens were loaded in the longitudinal direction. All experiments were fully reversed with a minimum temperature of $T_{\min} = 500^\circ\text{C}$. Maximum temperatures of $T_{\max} = 950^\circ\text{C}$ and $T_{\max} = 750^\circ\text{C}$ were utilized to study the effects of maximum temperature on damaging mechanisms and TMF life. A servohydraulic test frame with induction heating was used for all experiments. Axial displacements within the gage section were measured using a high temperature extensometer with 12.7 mm gage section. A 180 s cycle time was used with constant heating and cooling rates. K-type thermocouples spot welded to the ends of the gage section for the smooth specimens or near the notch on the notched specimens were utilized to provide a feedback signal for close-loop control of specimen temperature.

Experiments performed on smooth specimens were conducted in mechanical strain control in accordance with ASTM E2368-04 for thermomechanical fatigue testing. All notched specimen experiments were performed in force control and displacements across the gross notch section were measured using a high temperature extensometer with 12.7 mm gage length.

A crack initiation criterion was established to identify a crack depth of 0.5-1.0 mm for both mechanical strain-controlled and force-controlled experiments. For mechanical-strain controlled experiments (smooth specimens) a 10% load trend variation was used. As material hardening, softening or creep processes can result in a continuously changing load history, a 10% variation of the stabilized trend constitutes crack formation. For force-controlled experiments (notched specimens) an analogous method was implemented; initiation was defined when a 10% variation in the mechanical extensometer displacement signal occurred.

3. Results

3.1. Out-of-phase TMF 500°C↔950°C

OP TMF lives obtained in force control on smooth and circumferentially notched specimens are shown in Fig. 1. Notched specimens $k_t = 2$ and $k_t = 3$ follow the same life trend, indicating that increasing the notch severity beyond $k_t = 2$ is not more detrimental to OP TMF life. Experiments on the milder notch geometry $k_t = 1.3$ show that under the applied conditions, the effect of the notch is negligible as lives follow the smooth specimen life trend. Lives corresponding to $k_t = 1.7$ fall between the two bounds represented by the $k_t = 1/k_t = 1.3$ and $k_t = 2/k_t = 3$ trends.

Cracks that lead to final failure nucleated at a location away from the notch root, as shown in Fig. 2. Cracks nucleate furthest from the notch root in the bluntest notch, $k_t = 1.3$. The nucleation location approaches the notch root with increasing notch severity.

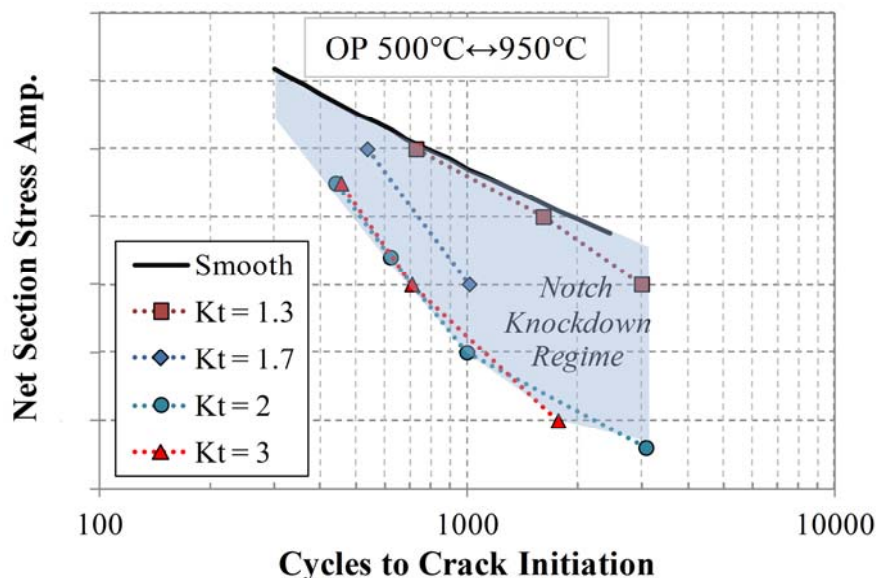


Figure 1. Crack initiation life under 500°C ↔ 950°C OP TMF for each notched specimen geometry.

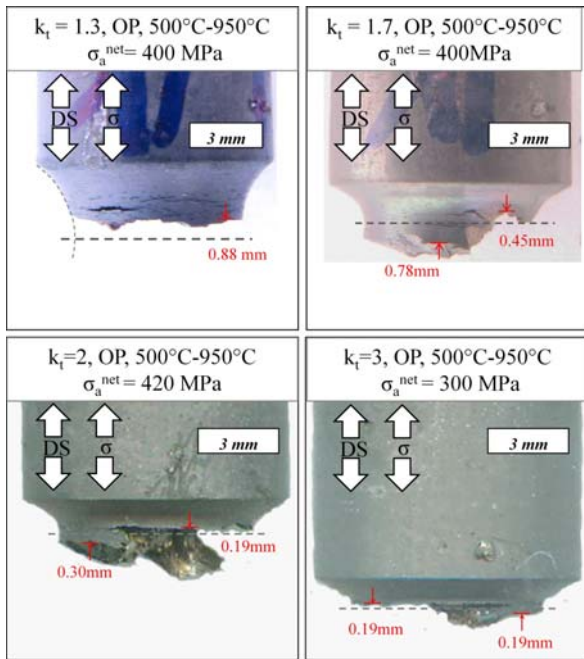


Figure 2. Fracture images indicating the location of crack initiation relative to the notch root.

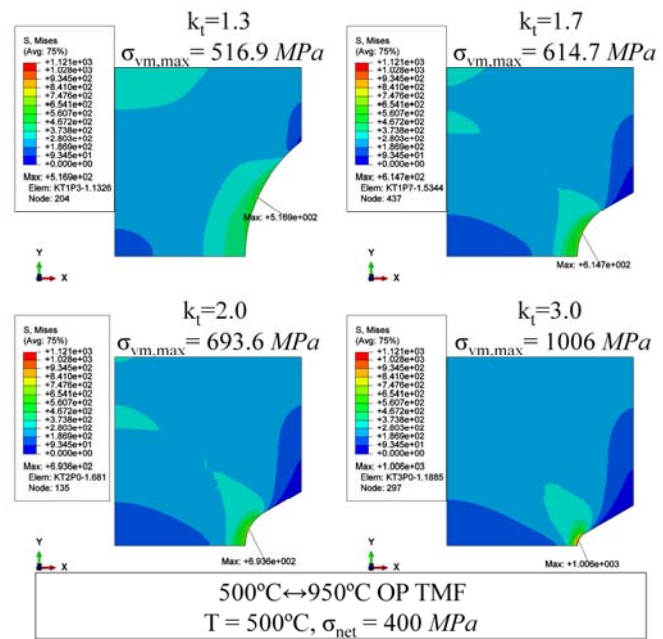


Figure 3. Von Mises equivalent stress at minimum temperature (tensile load).

The local notch response was predicted using a continuum based constitutive model within the ABAQUS finite element framework [7]. A model taking into account plasticity and creep was not available for the alloy studied and instead a transversely isotropic viscoplasticity model corresponding to another DS Ni-base superalloy was used [8]. The alloy studied exhibits higher yield strength in the virgin condition and a lower modulus. Nevertheless both superalloys exhibit the characteristic increase in yield strength around 750°C followed by a sharp decrease in strength. As such numerical results should be adequate for qualitative comparison.

The finite element meshes utilize linear quadrilateral elements throughout the domain. The cylindrically notched specimens were modeled using axisymmetric boundary conditions along with symmetry conditions at the net section to reduce the model to a quarter cross section of the extensometer gage section. A uniform pressure was applied to the top surface corresponding to the applied force. All TMF simulations of notched geometries were performed by first prescribing the mean temperature with no applied pressure. Then three reversals were applied, first loading to maximum temperature and applying the corresponding force for either OP or IP loading. Under the first peak force at elevated temperature, a great deal of initial yielding and hardening occurs. As such the cyclic response is taken as the final two reversals which better represent steady-state cyclic loading.

The stress responses at minimum temperature under the same OP TMF conditions are shown in Fig. 3. for an applied 400 MPa net section stress. The location of maximum von Mises stress during peak tension begins away from the notch root but approaches it with increasing notch severity. Similarly, the location of maximum equivalent inelastic cyclic strain approaches the notch root with increasing notch severity [9].

3.2. In-phase TMF 500°C↔950°C

Results from IP TMF are shown in Fig. 4 with the OP TMF knockdown regime region shown for

comparison. IP TMF lives of the $k_t = 1.3$ notch follow the smooth trend. This indicates that under IP TMF, as well as OP TMF, the $k_t = 1.3$ notch does not have a significant detrimental effect on TMF fatigue life.

3.3. Out-of-phase TMF $500^\circ\text{C} \leftrightarrow 750^\circ\text{C}$

The influence on initiation life from reducing the maximum temperature under OP TMF to 750°C is shown in Fig. 5. Even under the lower applied maximum temperature, notch geometries $k_t = 2$ and $k_t = 3$ follow the same life trend. Additional experiments within this temperature regime show that notch geometry $k_t = 1.3$ displays a small decrease in life compared to the smooth trend and $k_t = 1.7$ is slightly less damaging than exhibited by $k_t = 2 / k_t = 3$.

Under $T_{\max} = 750^\circ\text{C}$ OP TMF, some oxidation is present along interdendritic regions and grain boundaries, but overall the contribution from environmental processes is small. Under higher temperature $T_{\max} = 950^\circ\text{C}$ OP TMF, several secondary fatigue-environmental cracks oriented perpendicularly to the applied load are observed. There is no evidence of environmental-fatigue secondary cracks under IP TMF as seen under OP TMF.

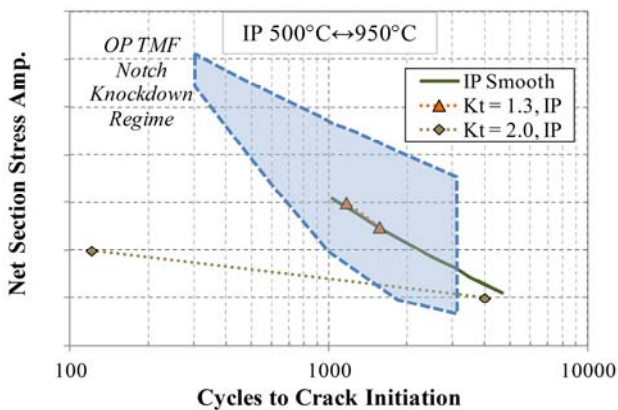


Figure 4. Crack initiation life under $500^\circ\text{C} \leftrightarrow 950^\circ\text{C}$ IP TMF for each notched specimen geometry.

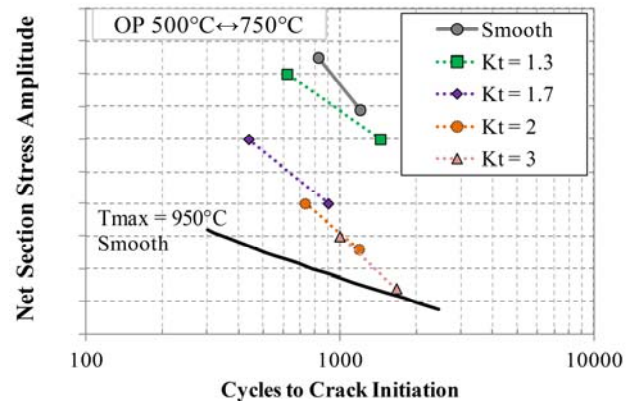


Figure 5. Crack initiation life under $500^\circ\text{C} \leftrightarrow 750^\circ\text{C}$ OP TMF for each notched specimen geometry.

4. Implications for life modeling

Most life modeling approaches tend to predict that increases in notch severity result in lower lives. It is apparent that a nonlocal approach will be needed to evaluate notched lives under TMF to predict the experimental results. In the next exercise, we evaluate some popular domain averaging schemes [10-14] to determine what methods work best in predicting the observed trends in lives. Here, we focus on OP TMF under $500^\circ\text{C} \leftrightarrow 950^\circ\text{C}$ to maintain a constant mechanism of damage. As shown earlier, the crack nucleation locations under OP TMF loading coincide well with the maximum von Mises stress and equivalent inelastic strain range. To keep the damage model simple for evaluation, a generalized energy-based damage parameter [15] that couples these two drivers is used,

$$D_o = \Delta \varepsilon_e^{in} \sigma_{e,\max} \quad (1)$$

where $\Delta \varepsilon_e^{in}$ is the equivalent inelastic strain range and $\sigma_{e,\max}$ is the maximum value of the von Mises equivalent stress over one cycle which occurs in tension for OP TMF. Since the loading is uniaxial, the loading in the vicinity of the notch is approximately proportional and hence using equivalent values is acceptable for this exercise for ease of computation.

As a baseline, the maximum D_o parameter for each geometry and applied load is shown in Fig. 6. As expected, this local approach gives high values for the D_o parameter and is highly conservative [3, 10-14, 16]. The local approach incorrectly predicts increasing damage with increasing notch severity, which is totally inconsistent with the observed experimental lives. A regression analysis using a power law relationship was used to attempt to correlate the maximum D_o parameter to lives, as shown in Fig. 7. This procedure does not collapse the life data.

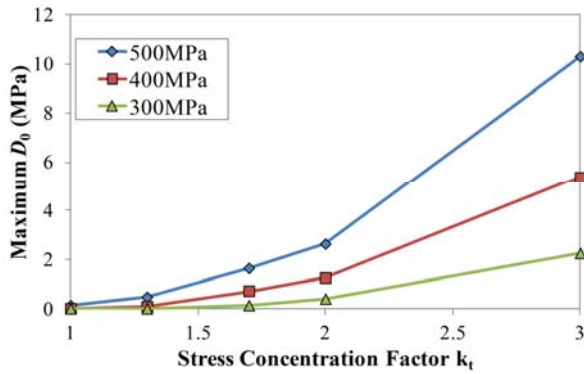


Figure 6. Maximum D_o parameter for all specimen geometries $500^\circ\text{C} \leftrightarrow 950^\circ\text{C}$ OP TMF.

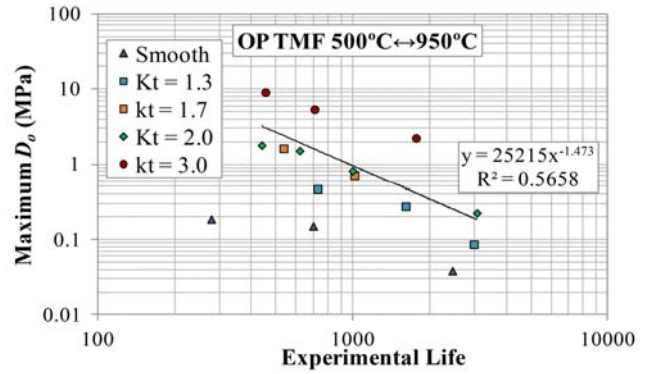


Figure 7. Correlation of maximum D_o parameter with experimentally determined OP TMF lives.

Rather than utilizing a local maximum quantity, nonlocal approaches utilize an averaged quantity over a domain or a point some distance away from the maximum. The simplest implementation is utilizing a point value some critical distance away from a key local quantity. Nonlocal quantities include averaging domains over a line, area or within a volume. The averaged generalized damage parameter can be defined as,

$$\bar{D}_o = \frac{1}{D} \int_D D_o dD \quad (2)$$

where D is the averaging domain; line, area or volume. Nonlocal approaches on isotropic materials typically utilize a line or point method as the response is centered about the notch root [10-12, 14]. However, for the transversely isotropic response of directionally-solidified (DS) alloys when loaded longitudinally, cracks are observed to initiate away from the notch root. Additionally the maximum equivalent inelastic strain range and maximum von Mises stress occur away from the notch root and the response changes during loading, with temperature, applied load level and across specimen geometries. Directions of relevant spatial gradients change with applied conditions and do not coincide with surface normals or crystallographic directions. As such an area averaging approach was used on the response predicted by the axisymmetric finite element method. As the domain represents an axisymmetric volume, in this case this is also equivalent to a volume averaging scheme.

A critical area approach [11, 13] was first evaluated for determining the integration domain. This method identifies the domain within which the damage quantity is a percentile of the maximum value,

$$A_{crit} = A(D_o \geq P \cdot \max \{D_o\}) \quad (3)$$

where A is the total area of the section of interest, A_{crit} is the critical area and P is a value between 0 and 1 that represents the percentile quantity used to define the critical domain. The critical area for all notch geometries based on 95-percentile ($P = 0.95$) under a 500 MPa applied net section stress is shown in Fig. 8. The size of the critical area decreases with increasing notch severity due to increases in the spatial gradients in the damage parameter.

The area averaged damage parameter using a 95-percentile area domain is shown in Fig. 9 for each notch geometry and three applied net section stresses. This method exhibits similar trends as using the local damage approach; increases in notch severity always produce additional damage in conflict with experimental observations.

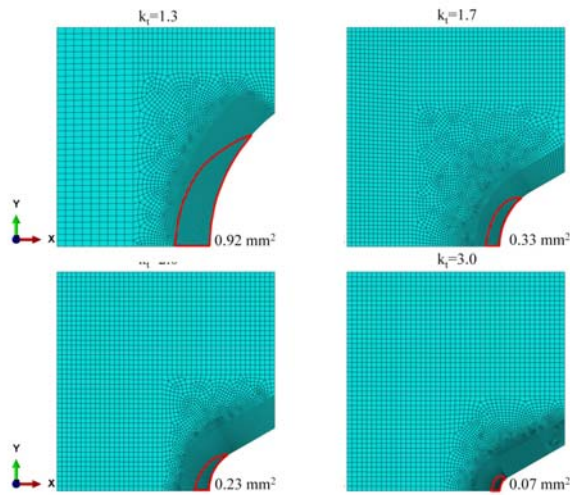


Figure 8. OP TMF 500°C ↔ 950°C
95-percentile critical areas based on D_o
parameter.

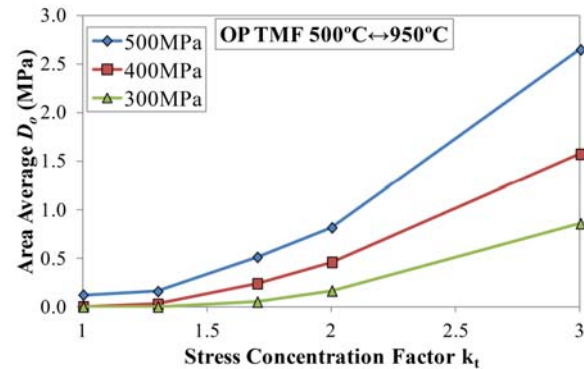


Figure 9. Nonlocal 95-percentile critical area \bar{D}_o
as a function of applied load and stress
concentration.

Invariant averaging domains have been used successfully in notch and component analysis [11, 12, 16]. For evaluating this approach, two methods are implemented: (1) a surface-sweep of the notch surface into the component as seen in Fig. 10(a) and (2) a circular-sweep within the component centered about the location of the maximum damage parameter shown in Fig. 10(b). An iterative method was utilized to achieve the desired critical area domain for each component as the axisymmetric component areas are irregular. A bisection zero finding method was implemented to reduce the residual $R_i = |A_{crit} - A(L_i)|$ to a satisfactory tolerance by iterating on the critical length L .

The area scale was parametrically varied to achieve an optimum domain for the largest net section stress amplitude case as shown in Fig. 11. Increasing the averaging area decreases the area average damage parameter as one might expect. As the averaging area increases, the difference in the driver between $k_t = 2$ and $k_t = 3$ lives becomes indistinguishable which is consistent with

experimental observations. Hence, both experimentally observed notch life sensitivity trends at low and high notch severity values are captured simultaneously with a single parameter variation.

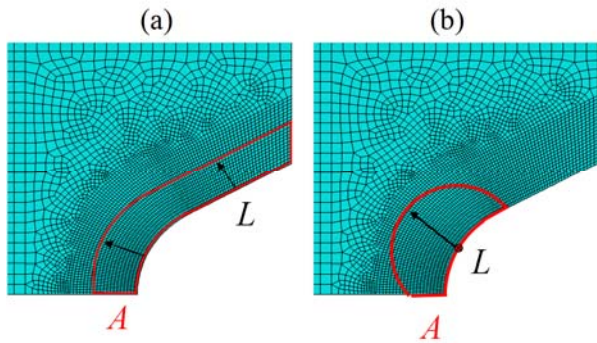


Figure 10. Domain for area averaging $k_t = 2.0$ notch using (a) surface-sweep method and (b) circular-sweep method.

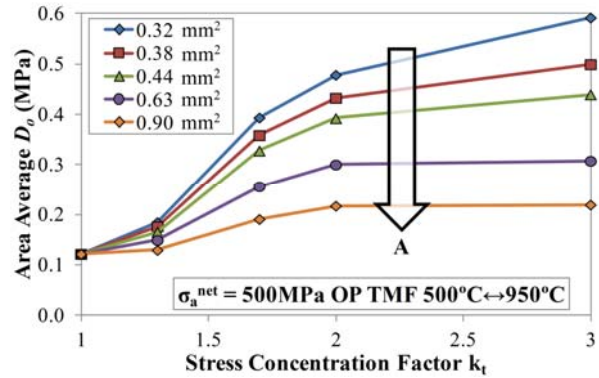


Figure 11. Surface-sweep nonlocal average \bar{D}_0 parameter for OP TMF under 500 MPa net section stress for increasing area domain.

Optimal areas for predicting $k_t = 1/k_t = 1.3$ and $k_t = 2/k_t = 3$ OP TMF notch life sensitivity trends were found to be 0.90 mm^2 and 0.77 mm^2 for surface-sweep and circular-sweep domains, respectively. The sweeping length scale, L , is shown for each method and notch geometry in Table 1.

Table 1. Sweeping Length Scales for Optimized Area Domains

Surface-Sweep		Circular-Sweep	
k_t	L (μm)	k_t	L (μm)
1.3	276	1.3	686
1.7	386	1.7	670
2	413	2	678
3	476	3	735

The surface-sweep scale is smaller than the circular-sweep scale as the sweeping area is performed over the entire notch surface length. The length scale changes to preserve the same size area for averaging the damage parameter in each notch geometry. Relevant length scales here are larger than the $200 \mu\text{m}$ length scale for point and line methods utilized by Moore and Neu for isothermal fatigue of the some notch geometry and material [16]. Naik et al. [14] found the line average domain to be between $20 \mu\text{m}$ and $100 \mu\text{m}$ for notched Ti-6Al-4V with stress concentrations varying between 2 and 4. For a notched Al alloy, Susmel and Taylor [12] utilized a $244 \mu\text{m}$ length scale for implementing a point method approach and a $154 \mu\text{m}$ length scale for a line method approach. In the same study Susmel and Taylor also investigated low-carbon steel and utilized $492 \mu\text{m}$ and $396 \mu\text{m}$ scales for point and line methods, respectively. It is critical to note however that the length scales obtained from the literature were determined from a line-method approach, whereas here an area method approach is utilized. As such it is expected that the scale will be larger here. Additionally, as the columnar grain size is fairly large in this alloy, and hence the relevant length scale can be expected to be on the same order as the grain size (0.2 mm to 1.0 mm).

The correlation of the area averaged damage parameter with experimental OP TMF life is shown in Fig. 12. Both averaging methods improve the life predictability as compared against the local method and critical area nonlocal approaches presented previously. With the exception of one life

value, all predictions are within a factor of two utilizing either averaging method.

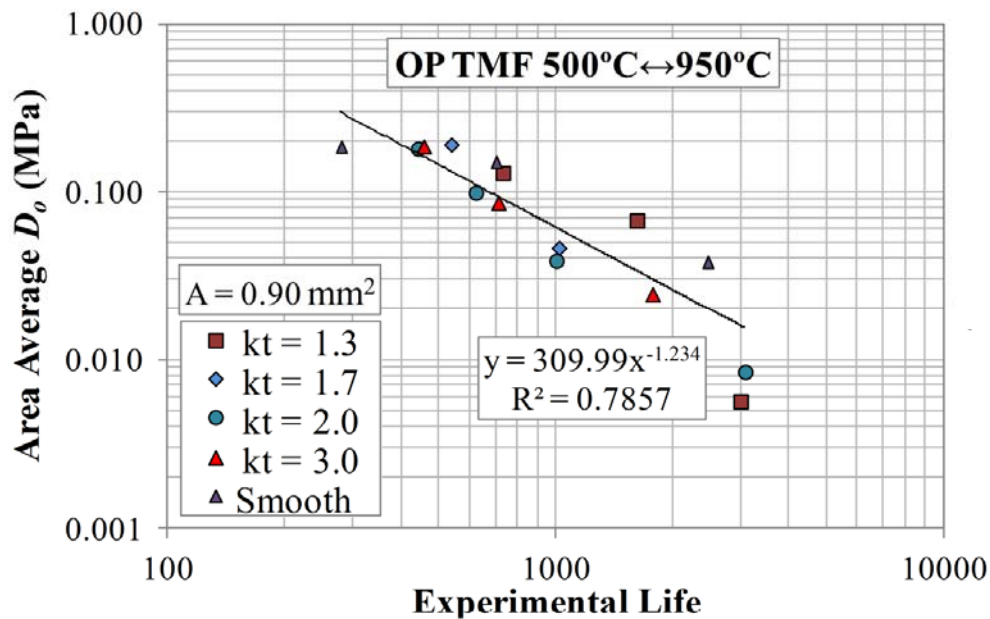


Figure 12. Correlated nonlocal \bar{D}_o against experimentally determined OP TMF lives using the invariant area surface sweep method.

5. Conclusions

- For OP TMF $500^{\circ}\text{C} \leftrightarrow 950^{\circ}\text{C}$, the $k_t = 1.3$ notch represents the lower bound of fatigue notch sensitivity as there is no appreciable knock-down in life relative to the smooth life trend. For $k_t \geq 2$, the fatigue life is also insensitive to the severity of the notch. The $k_t = 1.7$ notch falls in between the $k_t = 1/k_t = 1.3$ and $k_t = 2/k_t = 3$ trends.
- In DS alloys loaded longitudinally, the OP TMF cracks in notched specimens nucleate away from the notch root. The nucleation location approaches the notch root with increasing notch severity and increasing applied force amplitude for a given notch geometry. These trends are captured in a computational stress-strain analysis using either von Mises equivalent stress or the cyclic inelastic equivalent strain range cyclic response parameters.
- For OP TMF with smaller maximum temperature, $500^{\circ}\text{C} \leftrightarrow 750^{\circ}\text{C}$, the $k_t = 1.3$ notch exhibits a small knock-down in life relative to the smooth life trend. The $k_t = 1.7$ notch falls in between the $k_t = 1.3$ and $k_t = 2/k_t = 3$ life trends.
- Under IP TMF $500^{\circ}\text{C} \leftrightarrow 950^{\circ}\text{C}$, the $k_t = 1.3$ notch also follows the smooth specimen life trend similar to OP TMF.
- Neither local nor critical-domain nonlocal methods adequately collapsed notched and smooth OP TMF $500^{\circ}\text{C} \leftrightarrow 950^{\circ}\text{C}$ life data.
- A nonlocal invariant area-averaging method was utilized to collapse all experimental data that included variations in notch severity and force amplitude onto a single trend. Two schemes were implemented to define the invariant area-averaging domain; one based on the maximum value of the generalized damage parameter and a circular sweep of the surrounding domain and another based on the domain around the entire notch surface. Both methods worked reasonably well.

Acknowledgements

This effort was supported by Siemens Energy Inc., Orlando, FL. The interactions with Phillip Gravett, Sachin Shinde, and Saiganesh Iyer are appreciated.

References

- [1] Z. Mazur, A. Luna-Ramirez, J.A. Juarez-Islas, A. Campos-Amezcu, Failure analysis of a gas turbine blade made of Inconel 738LC alloy. *Eng Failure Analysis*, 12 (2005) 474-486.
- [2] R.C. Reed, *The Superalloys - Fundamentals and Applications*, Cambridge, 2006.
- [3] E. Mazza, M. Hollenstein, S. Holdsworth, R.P. Skelton, Notched specimens thermo-mechanical fatigue of a 1CrMoV turbine steel. *Nuclear Eng Design*. 234 (2004) 11-24.
- [4] F. Colombo, E. Mazza, S.R. Holdsworth, R.P. Skelton, Thermo-mechanical fatigue tests on uniaxial and component-like 1CrMoV rotor steel specimens. *Int J Fatigue*, 30 (2008) 241-248.
- [5] R.A. Kupkovits, R.W. Neu, Thermomechanical fatigue of a directionally-solidified Ni-base superalloy: Smooth and cylindrically-notched specimens. *Int J Fatigue*, 32 (2010) 1330-1342.
- [6] Z.J. Moore, R.W. Neu, Creep-fatigue of a directionally-solidified Ni-base superalloy – smooth and cylindrically notched specimens. *Fatigue Fracture Eng Mater Struct*, 34 (2010) 17-31.
- [7] ABAQUS v6.9. Dassault Systèmes: Providence, RI, 2009.
- [8] M.M. Shenoy, D.L. McDowell, R.W. Neu, Transversely isotropic viscoplasticity model for a directionally solidified Ni-base superalloy. *Int J Plas*, 22 (2006) 2301-2326.
- [9] P. Fernandez-Zelaia, Thermomechanical Fatigue Crack Formation in Nickel-Base Superalloys at Notches, M.S. Thesis, Georgia Institute of Technology, Atlanta, GA, USA, 2012.
- [10] R. Mucke, H. Kiewel, Nonlocal cyclic life prediction for gas turbine components with sharply notched geometries. *J Eng Gas Turbines Power*, 130(1) (2008) 012506.
- [11] L. Susmel, D. Taylor, A novel formulation of the theory of critical distances to estimate lifetime of notched components in the medium-cycle fatigue regime. *Fatigue Fracture Eng Mater Struct*, 30 (2007) 567-581.
- [12] L. Susmel, D. Taylor, An elasto-plastic reformulation of the theory of critical distances to estimate lifetime of notched components failing in the low/medium-cycle fatigue regime. *J Eng Mater Technol*, 132(2) (2010) 021002.
- [13] D. Taylor, The theory of critical distances. *Eng Fracture Mechanics*, 75 (2008) 1696-1705.
- [14] R.A. Naik, D.B. Lanning, T. Nicholas, A.R. Kallmeyer., A critical plane gradient approach for the prediction of notched HCF life. *Int J Fatigue*, 27 (2005) 481-492.
- [15] W.J. Ostergren, A damage function and associated failure equations for predicting hold time and frequency effects in elevated temperature low cycle fatigue. *J Testing Evaluation*, 4 (1976) 327-339.
- [16] Z.J. Moore, R.W. Neu, Fatigue life modeling of anisotropic materials using a multiaxial notch analysis. *J Eng Mater Technol*, 133(3) (2011) 031001.